Supporting Information

Injectable Extracellular Matrix-mimetic Hydrogel Based on Electrospun Janus Fibers

Jinzhong Zhang, Xiaolong Zha, Gengxin Liu, Huipeng Zhao, Xiaoyun Liu,* and Liusheng Zha**

J. Zhang, L. Zha
State Key Laboratory for Modification of Chemical Fibers and Polymer Materials, College of Materials Science and Engineering, Donghua University, Shanghai 201620, China
E-mail: lszha@dhu.edu.cn

X. Zha
Trauma Center, Shanghai General Hospital, Shanghai Jiao Tong University School of Medicine, Shanghai 201620, China.
E-mail: m13524282806@163.com

G. Liu
State Key Laboratory for Modification of Chemical Fibers and Polymer Materials, Center for Advanced Low-dimension Materials, College of Material Science and Engineering, Donghua University, Shanghai201620, China

H. Zhao, X. Liu
Research Center for Analysis and Measurement, Donghua University, Shanghai 201620, China
E-mail: xyliu@dhu.edu.cn

Supplementary Figures and Discussion

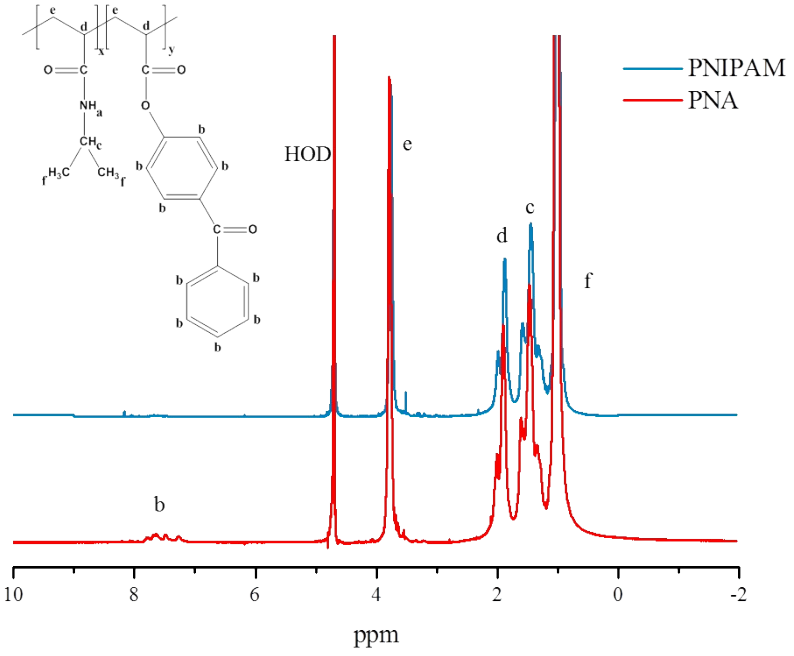

(a)

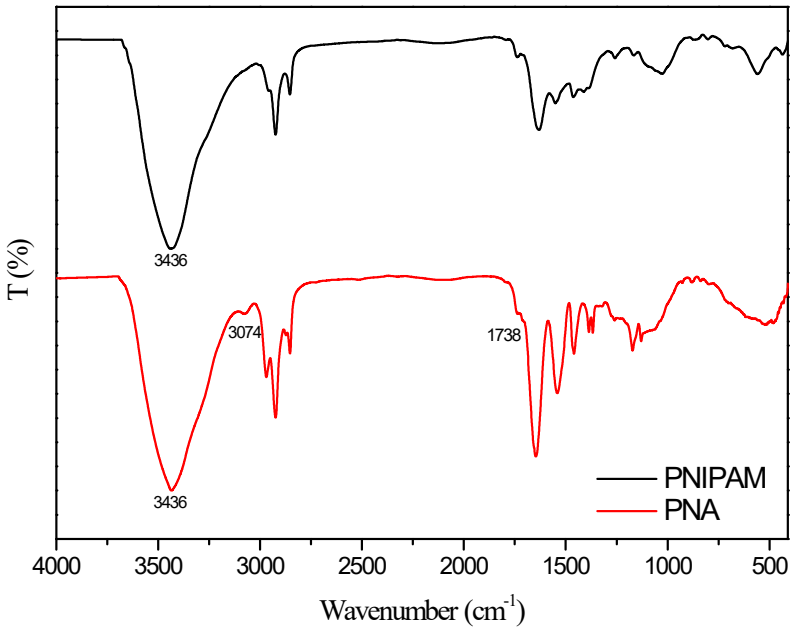

(b)

Fig. S1 ^{1}H NMR spectra (D_2O) (a) and FTIR spectra (b) of PNA and PNIPAM

By comparing ^{1}H NMR spectra of PNA and PNIPAM, it can be found that multiple peaks (b) within 7~8 ppm only appear in ^{1}H NMR spectrum of PNA, which indicates that ABP units are existent in PNA molecular chain. The relative areas of peaks b and e can be used to estimate the molar percentage of ABP units within the molecular chain of PNA, and the result is 1.10 mol%. By Comparing FTIR spectra of PNIPAM and PNA, the appearance of 1738 cm^{-1} and 3074 cm^{-1} peaks in FTIR spectrum of PNA, which are respectively attributed to stretching vibrations of ketone carbonyl group and C-H of benzene rings, also reveals that ABP units are existent in PNA molecular chain.

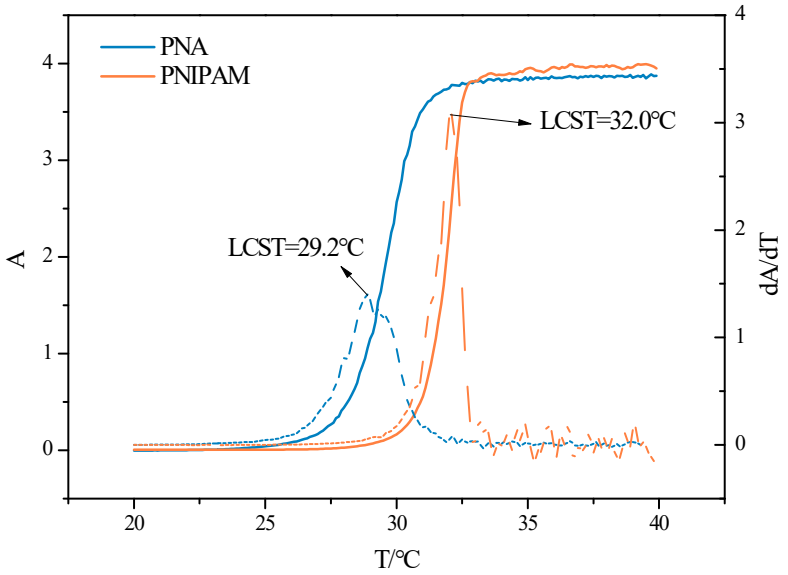

Fig. S2 The absorbance (A) of diluted PNA or PNIPAM aqueous solution at 500 nm at various temperatures (A~T) and their differential curves (dA/dT~T)

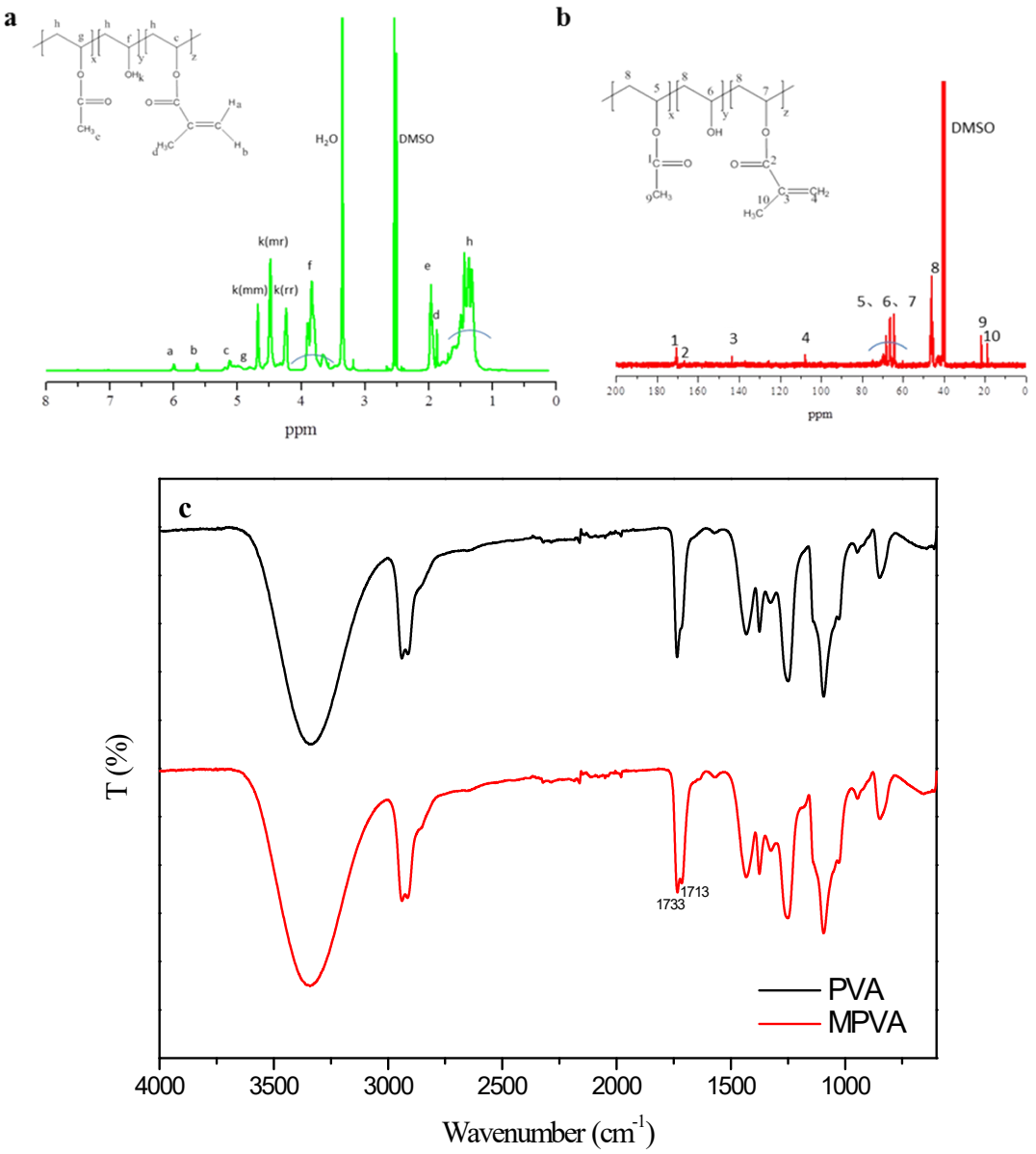

Fig. S3 (a) ^{1}H NMR and (b) ^{13}C NMR spectra of MPVA (d_6-DMSO) and (c) FTIR spectra of PVA and MPVA

The peaks (f, k) in (a) and the peak (6) in (b) are uniquely associated with the hydrogens and carbon of vinyl alcohol units, respectively, as marked in its structural formula. Since the alcoholysis degree of the PVA for preparing MPVA is 88%, the peaks (e, g) in (a) and the ones (1, 5, 9) in (b) are particularly attributed to the hydrogens and carbons of vinyl acetate units, respectively. The peaks (a, b, c, d) in (a) and the ones (2, 3, 4, 7, 10) in (b), which are not existent on ^{1}H NMR and ^{13}C NMR spectra (not given) of the PVA as raw material, should be associated with the hydrogens and carbons of vinyl methacrylate units formed after modifying PVA by GMA, respectively. Due to absence of the peaks related to the hydrogens or carbons of glycidyl group in (a) or (b), it is further confirmed that the reaction between PVA and GMA catalyzed by DMAP is transesterification. The content of vinyl methacrylate unit within MPVA chain can be calculated from relative areas of the peaks a, f and g, and the result is 1.05 mol%. By Comparing FTIR spectra of PVA and MPVA, the appearance of 1713 cm^{-1} peak in FTIR spectrum of MPVA should be attributed to carbonyl groups of vinyl methacrylate units existing within its molecular chain.

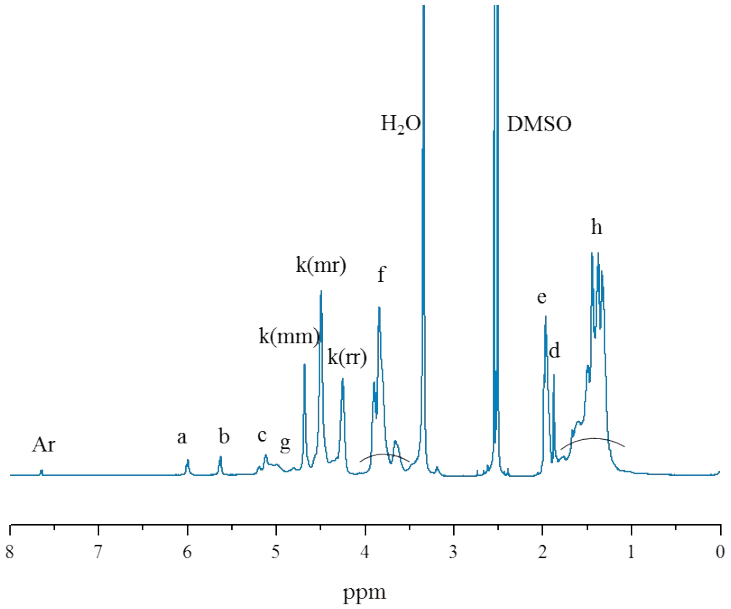

Fig. S4 ^{1}H NMR spectrum of FMPVA (DMSO-d_6)

In addition to containing the same peak as MPVA, the ^{1}H NMR spectrum of FMPVA shows a new chemical shift in the range of 7.8-8.0, and this shift can be considered as a proton peak in the aromatic ring (Ar) of the perylene group.

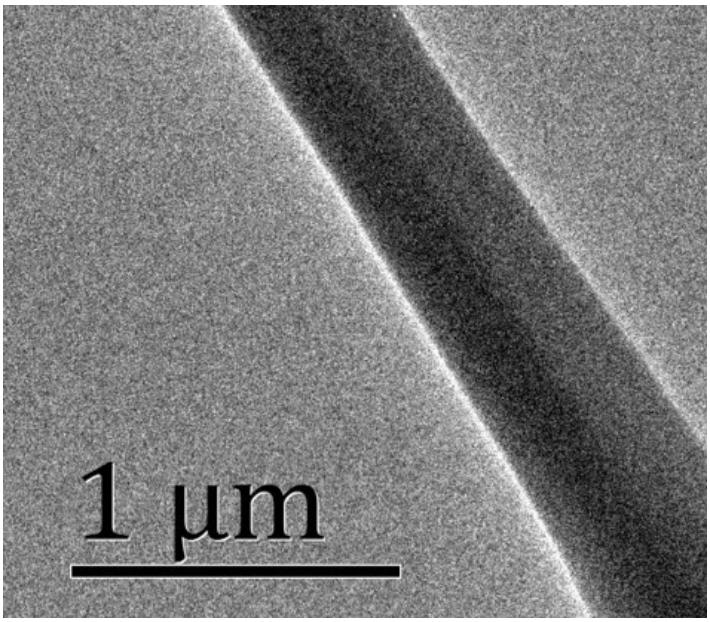

Fig. S5 TEM image of a typical of PNA/MPVA Janus nanofiber

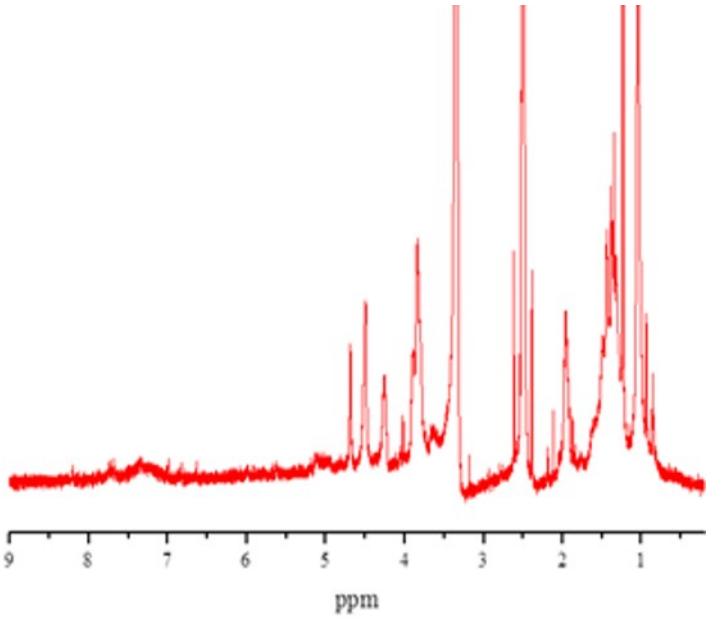

Fig. S6 ^{1}H NMR spectrum of shortened PNA/MPVA Janus nanofibers dispersed in DMSO-d_6

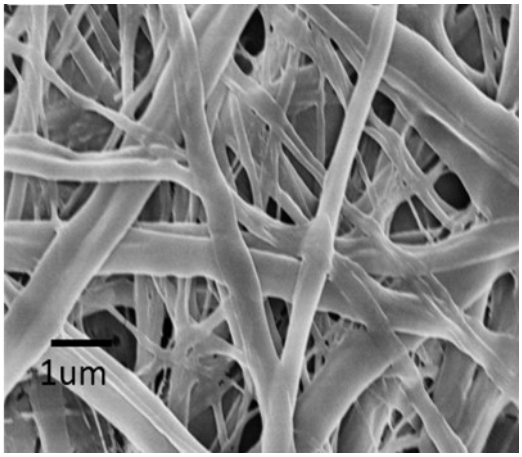

Fig. S7 SEM image of the PNA/MPVA Janus nanofibers after immersion in water at room temperature for 6 h and then drying at 105℃ for 12 h

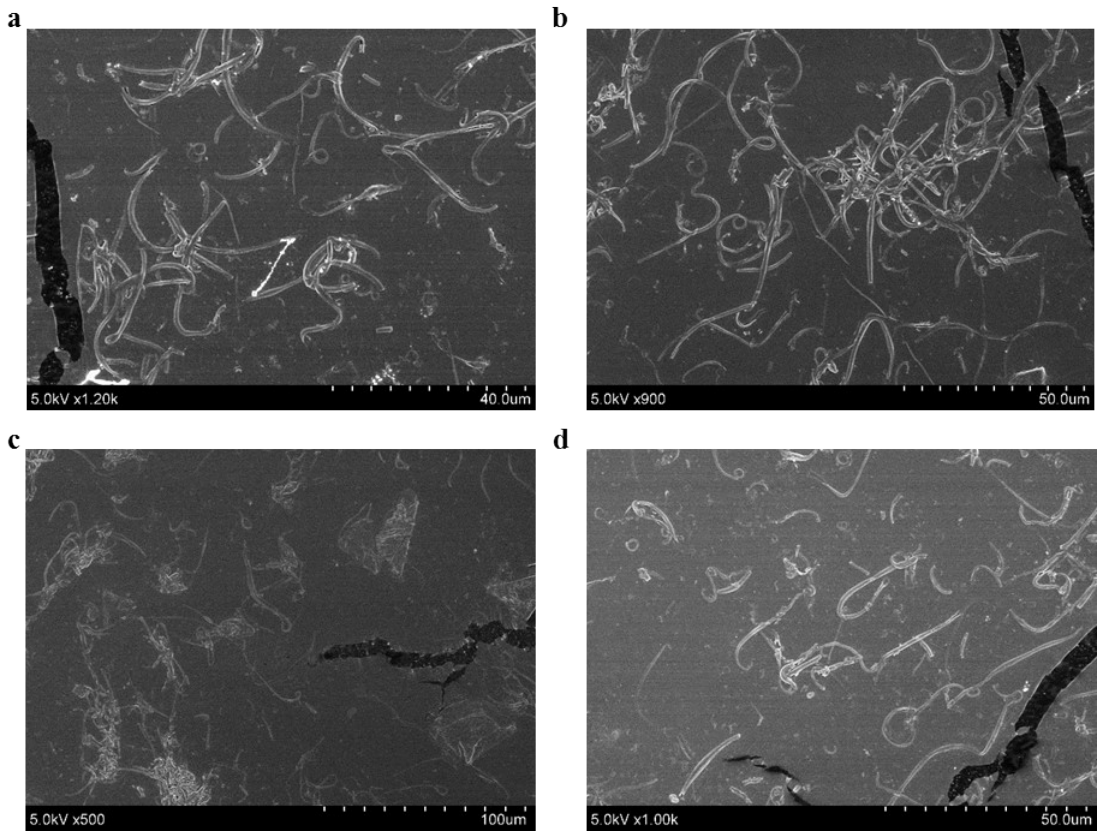

Fig. S8 a) SEM image of shortened PNA/MPVA Janus nanofibers in IEMH-3b. b) SEM image of shortened PNA/MPVA Janus nanofibers in IEMH-7b. c) SEM image of shortened PNA/MPVA Janus nanofibers in IEMH-5a. d) SEM image of shortened PNA/MPVA Janus nanofibers in IEMH-5c.

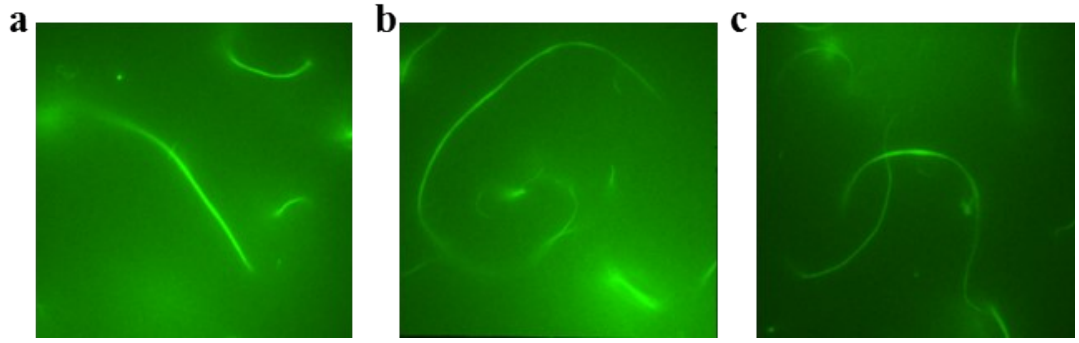

Fig. S9 TRIFM images of the dispersions of shortened PNA/FMPVA Janus nanofibers in pH 7.4 PBS with different concentrations. a) 0.08 wt%; b) 0.1 wt%; c)0.12 wt%

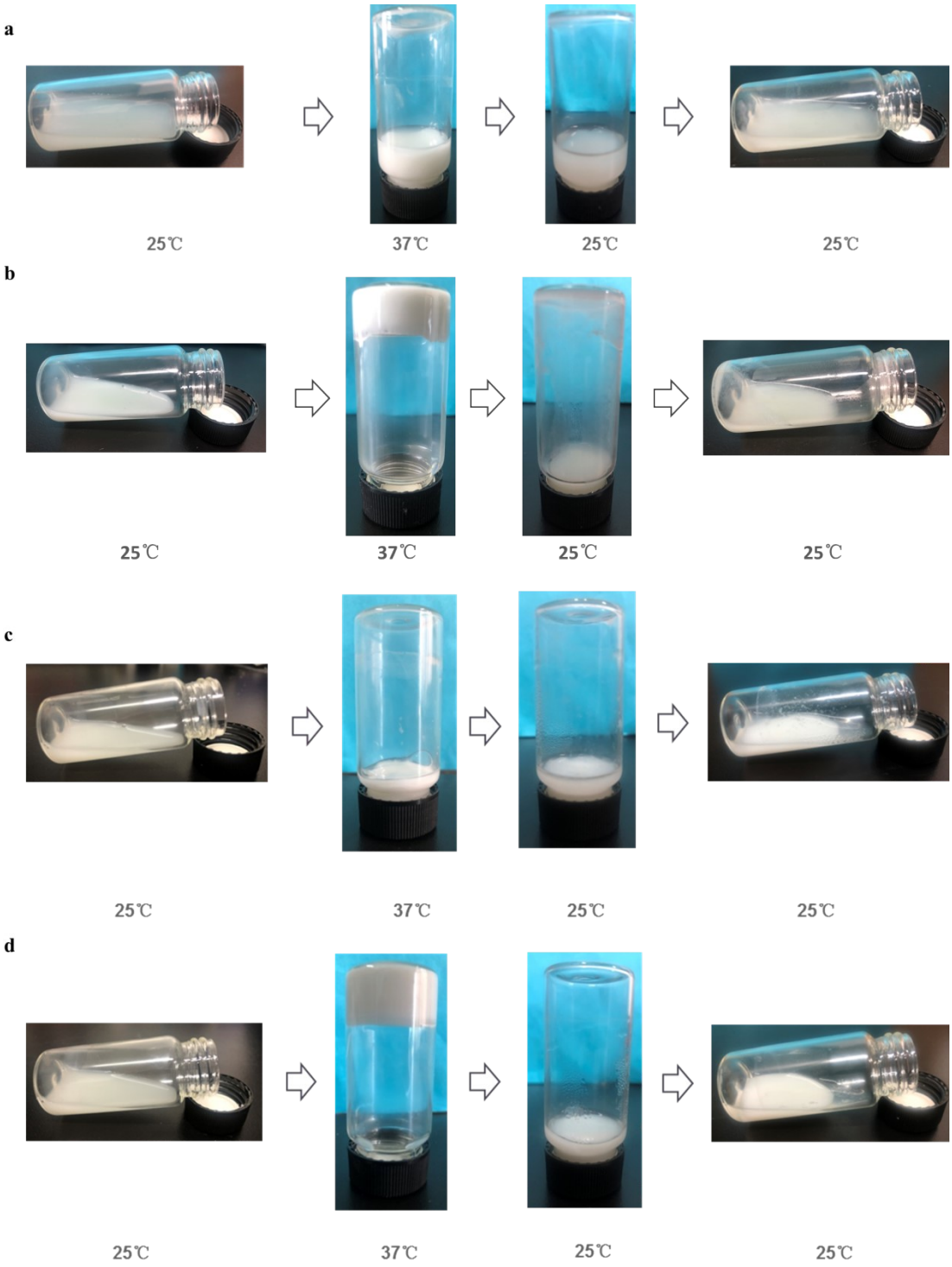
a
25℃
37℃
25℃
25℃
b
25℃
37℃
25℃
25℃
c
25℃
37℃
25℃
25℃
d
25℃
37℃
25℃
25℃

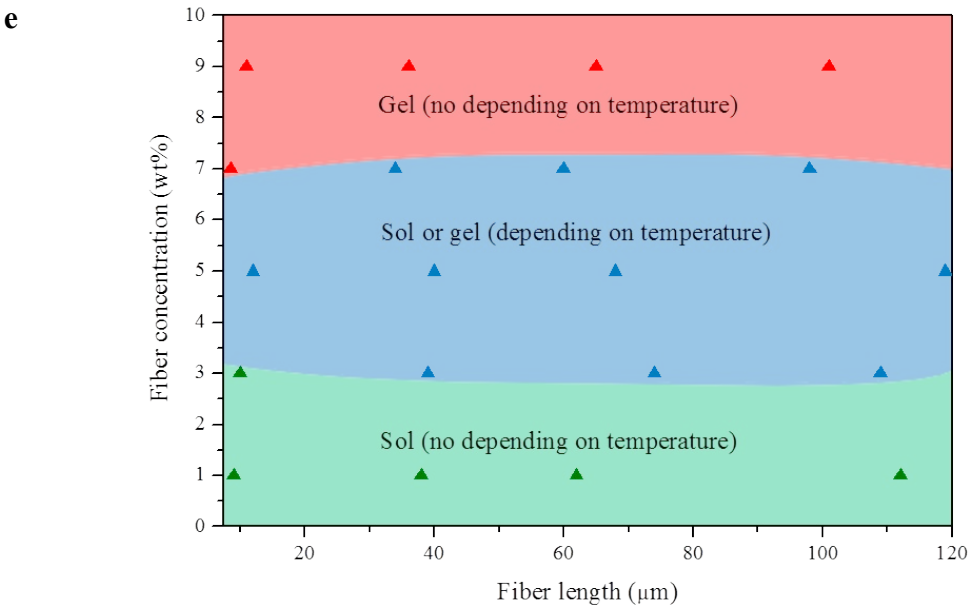

Fig. S10 Vial inversion test results. a) Optical images of inverted glass vials containing sample IEMH-3b below (25 °C) and above (37 °C) the gelation temperature. b) Optical images of inverted glass vials containing sample IEMH-7b below (25 °C) and above (37 °C) the gelation temperature. c) Optical images of inverted glass vials containing sample IEMH-5a below (25 °C) and above (37 °C) the gelation temperature IEMH-5a. d) Optical images of inverted glass vials containing sample IEMH-5c below (25 °C) and above (37 °C) the gelation temperature. e) Sol-gel phase diagram of IEMHs with fiber length and concentration as variables

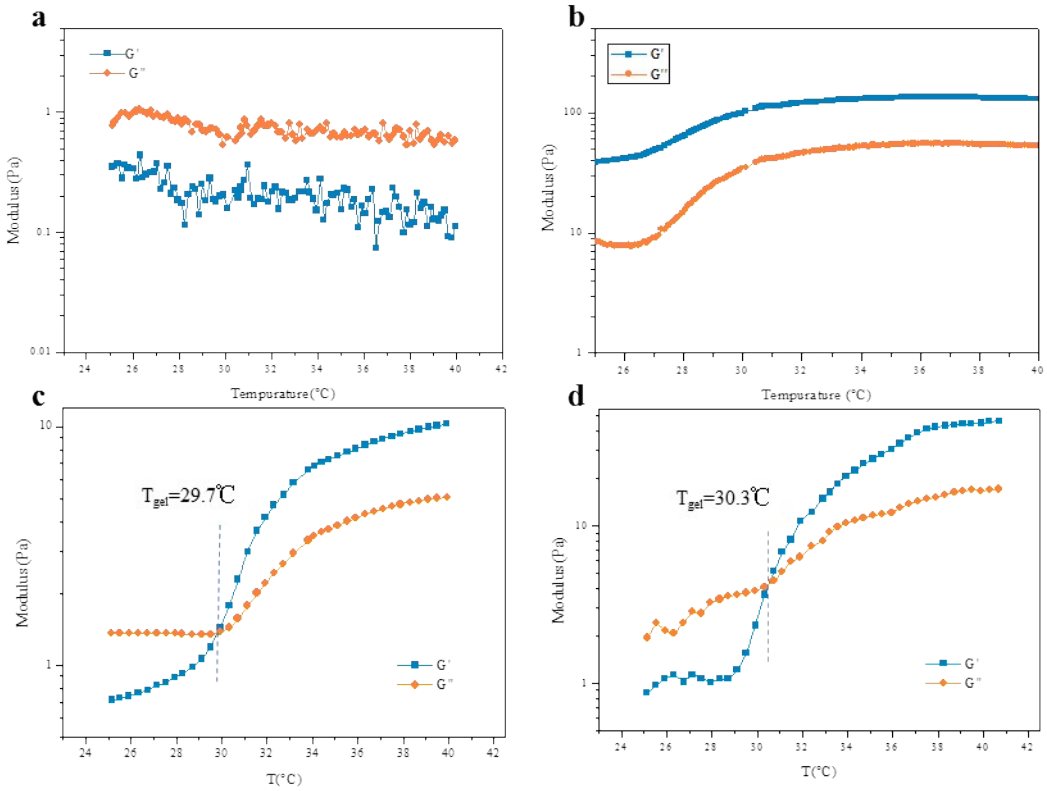

Fig. S11 Temperature dependent G' and G" of IEMHs measured at the oscillation frequency of 1 Hz and the heating rate of 1 °C/min over 25−40 °C temperature range. a) G′ and G″ of IEMH-3b as a function of temperature. b) G′ and G″ of IEMH-7b as a function of temperature. c) G′ and G″ of IEMH-5a as a function of temperature (The dashed line indicates where G′ and G″ intersect). d) G′ and G″ of IEMH-5c as a function of temperature (The dashed line indicates where G′ and G″ intersect)

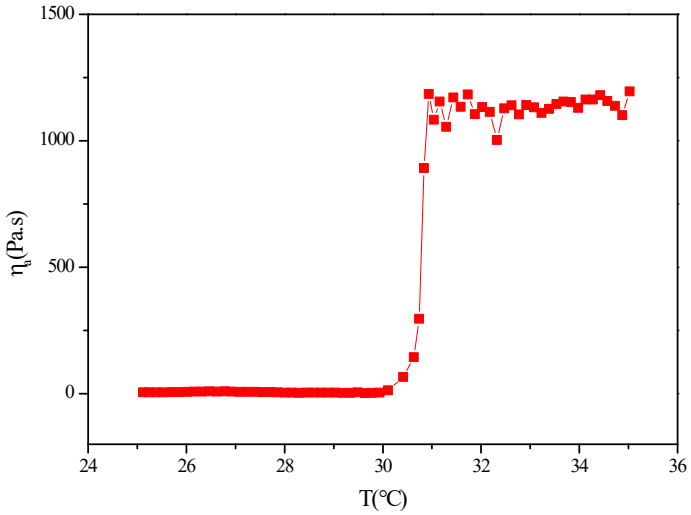

Fig. S12 The apparent viscosity (η_a) of IEMH-5b as a function of temperature (heating rate: 1 °Cmin^{-1} , shear rate: 1 s^{-1})

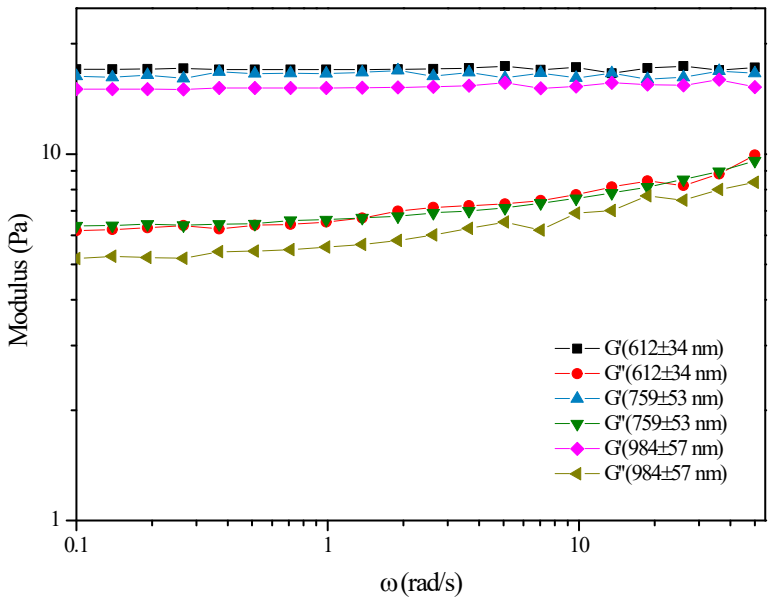

Fig. S13 G' and G" of three IEMHs of 5 wt% concentration of the PNA/MPVA Janus fibers with different diameters (612±34 nm, 759±53 nm and 984±57 nm) at 37 °C as a function of oscillation frequency

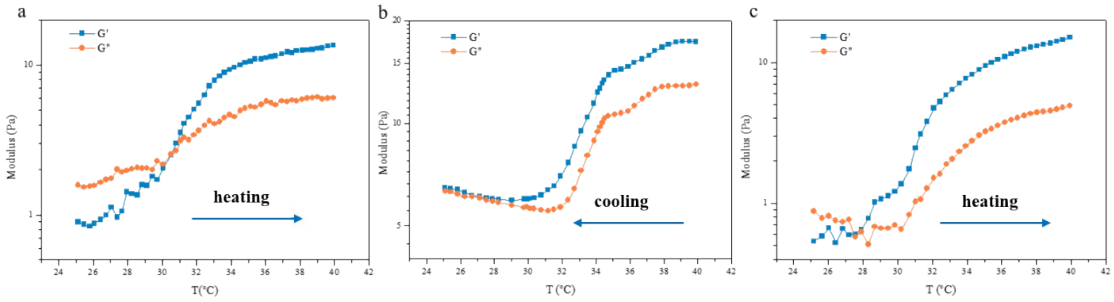

Fig. S14 Evolution of the dynamic moduli (G' and G") of IEMH-5b during a heating-cooling-heating cycle with the heating or cooling rate of 1 °C/min and the oscillation frequency of 1 Hz. a) heating from 25 °C to 40 °C, b) cooling from 40 °C to 25 °C. c) Heating from 25 °C to 40 °C

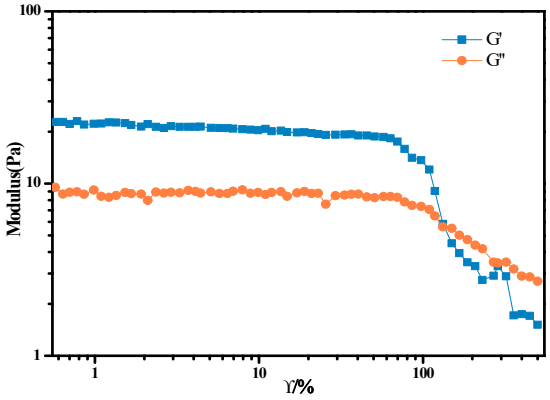

Fig. S15 G' and G" of IEMH-5b at 37 ℃ vs. strain (oscillation frequency:1Hz)

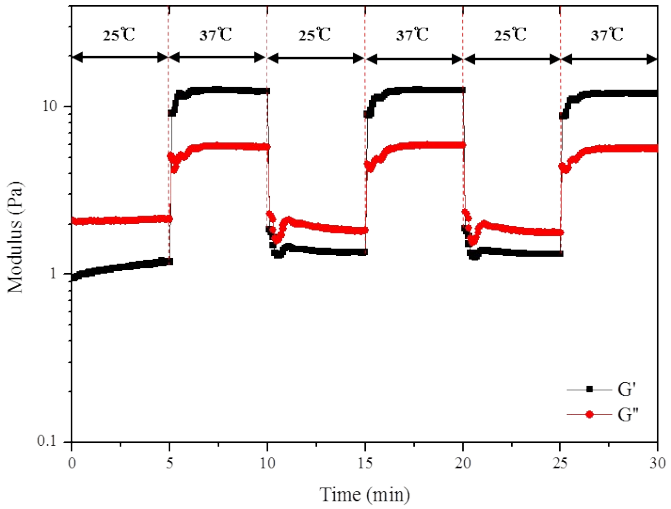

Fig. S16 Cyclic temperature step testing G' and G" of IEMH-5b between 25 ℃ and 37℃ (oscillation frequency: 1Hz)

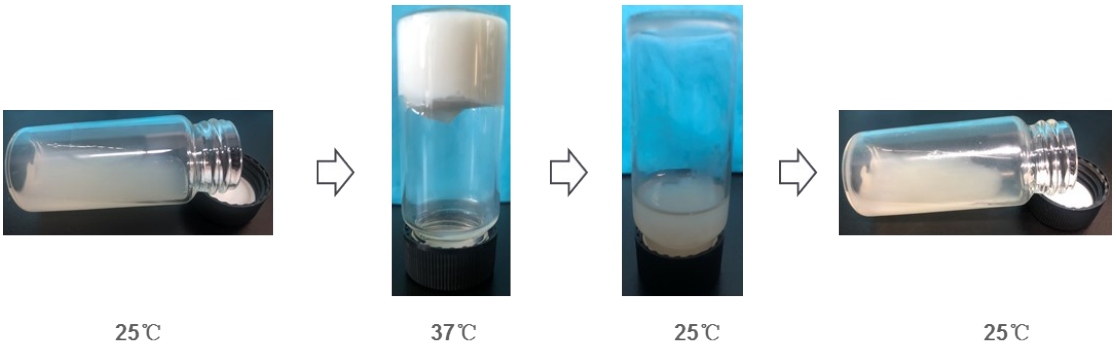

Fig. S17 Vial inversion test results of IEMH-p

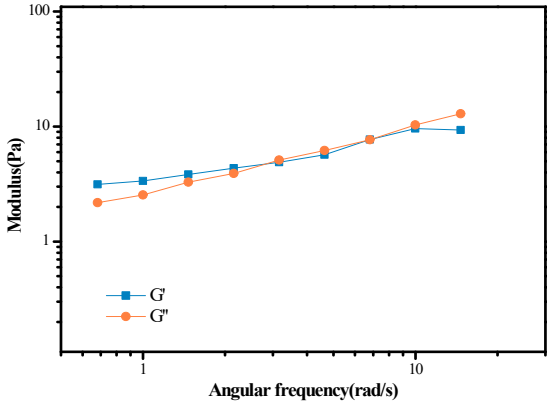

Fig. S18 G' and G" of IEMH-p at 37℃ as a function of oscillation frequency

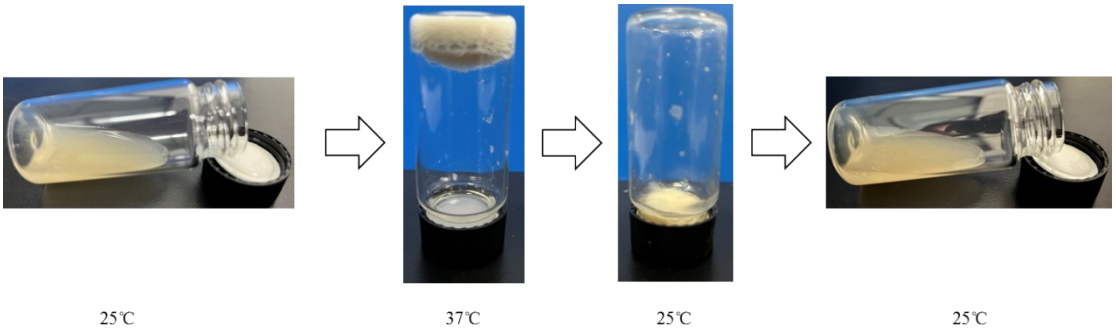

Fig. S19 Optical images of inverted glass vials containing the sample prepared using D_2O as solvent below (25 °C) and above (37 °C) the gelation temperature

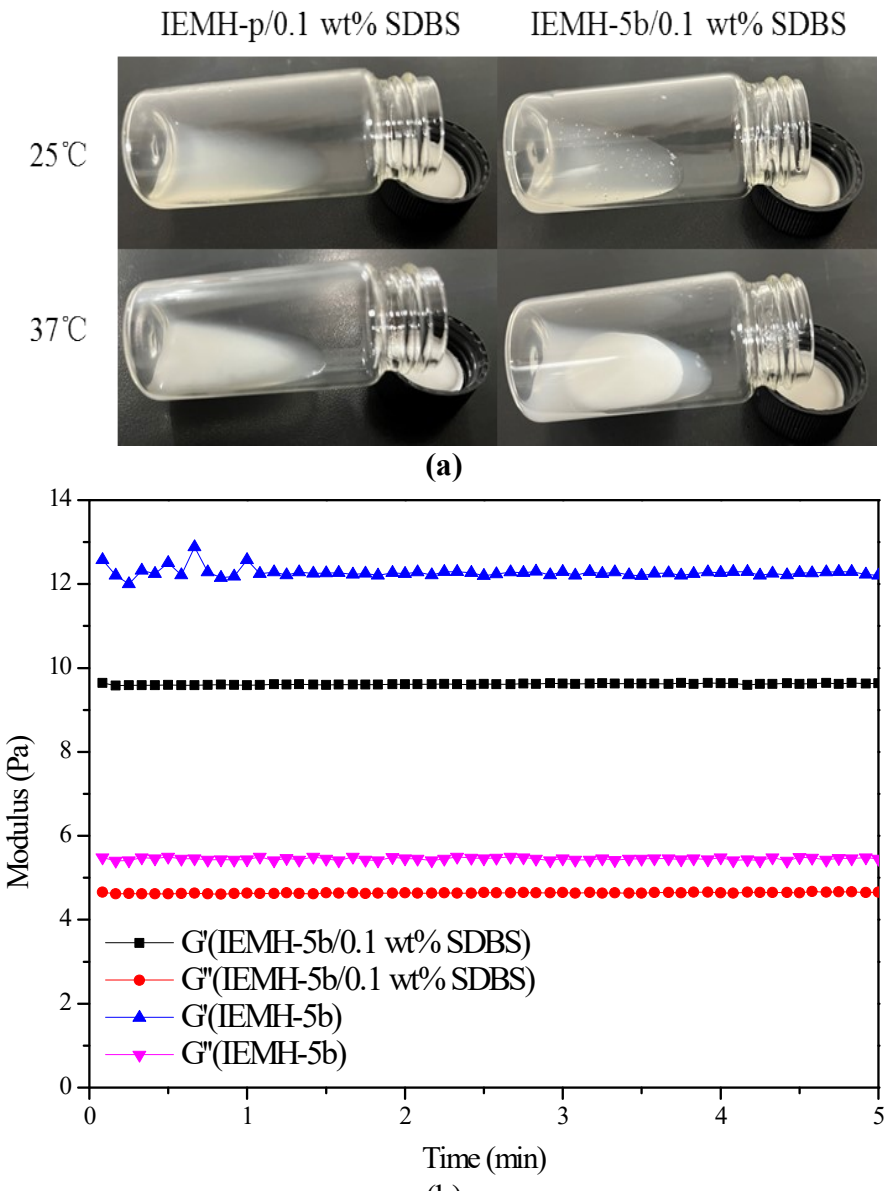

Fig. S20 a) Optical images of inverted glass vials containing IEMH-p/0.1 wt% SDBS or IEMH-5b/0.1 wt% SDBS at 25 °C and 37 °C. b) G' and G'' of IEMH-5b and IEMH-5b/0.1 wt% SDBS at 37°C as a function of time.

Table S1. The n of IEMHs

Sample code	IEMH-5a	IEMH-5b	IEMH-5c	IEMH-3b	IEMH-7b
n	0.39	0.62	0.71	0.68	0.40
r^2	0.99	0.97	0.96	0.95	1.00